Extracellular vesicles shed by follicular lymphoma B cells promote the polarization of bone marrow stromal cell niche

Erwan Dumontet, Céline Pangault, David Roulois, Matthis Desoteux, Simon Léonard, Tony Marchand, Maelle Latour, Patricia Legoix, Damarys Loew, Florent Dingli, et al.

Extracellular vesicles shed by follicular lymphoma B cells promote the polarization of bone marrow stromal cell niche

Erwan Dumontet[1,2], Céline Pangault[1,2], David Roulois[1], Matthis Desoteux[3], Simon Léonard[1], Tony Marchand[1,4], Maelle Latour[1,2], Patricia Legoix[5], Damarys Loew[6], Florent Dingli[6], Joelle Dulong[1,2], Erwan Flecher[7], Cédric Coulouarn[3], Guillaume Cartron[8], Thierry Fest[1,2], and Karin Tarte[1,2]

[1] UMR_ S 1236, INSERM, Univ Rennes, EFS Bretagne, LabEx IGO, F-35000 Rennes, France

[2] CHU de Rennes, Department of Biology, F-35000 Rennes, France

[3] UMR_S 1242 Chemistry Oncogenesis Stress Signaling (COSS), INSERM, Univ Rennes, Centre de Lutte contre le Cancer Eugène Marquis, F-35000 Rennes, France

[4] CHU de Rennes, Department of Hematology, F-35000 Rennes, France

[5] Institut Curie Genomics of Excellence (ICGex) Platform, Institut Curie Research Center, PSL Research University, F-75005, Paris, France

[6] Laboratoire de Spectrométrie de Masse Protéomique, Institut Curie Research center, PSL Research University, F-75005, Paris, France

[7] CHU de Rennes, Department of Thoracic and Cardiac Surgery, F-35000 Rennes, France

[8] Department of Hematology, CHU Montpellier, F-34000, Montpellier, France

Running title: Extracellular vesicles and follicular lymphoma

Scientific category: LYMPHOID NEOPLASIA

Correspondence

Karin Tarte, INSERM, UMR U1236, Faculté de Médecine, 2 Avenue du Pr Léon Bernard, F-35043 Rennes; e-mail: karin.tarte@univ-rennes1.fr. Phone: +33 (0) 223 234 512

KEY POINTS

1. FL-derived extracellular vesicles (EVs) impact bone marrow stromal cell phenotype and favor their B-cell supportive activity

2. The gene expression profile of bone marrow FL B cells supports a specific network of interactions with EV-primed bone marrow stromal cells

ABSTRACT

Follicular Lymphoma (FL) originates in the lymph nodes (LN) and infiltrates bone marrow (BM) early in the course of the disease. BM FL B cells are characterized by a lower cytological grade, a decreased proliferation, and a specific phenotypic and subclonal profile. Mesenchymal stromal cells (MSC) obtained from FL BM display a specific gene expression profile (GEP), including enrichment for a lymphoid-stromal cell signature, and an increased capacity to sustain FL B-cell growth. However, the mechanisms triggering the formation of the medullar FL permissive stromal niche have not been yet identified. In the current work, we demonstrated that FL B cells produced extracellular vesicles (EVs) that could be internalized by BM-MSC, making them more efficient to support FL B-cell survival and quiescence. Accordingly, EVs purified from FL BM plasma activated TGF-β dependent and independent pathways in BM-MSC, modified their GEP, triggering an upregulation of factors classically associated with hematopoietic stem cell niche, including CXCL12 or angiopoietin-1. Moreover, we provided the first characterization of BM FL B-cell GEP, allowing the definition of the landscape of molecular interactions they could engage with EV-primed BM-MSC. This work identified FL-derived EVs as putative mediators of BM stroma polarization and supported further investigation of their clinical interest for targeting the crosstalk between BM-MSC and malignant B cells.

INTRODUCTION

Follicular Lymphoma (FL) is the most common indolent B-cell lymphoma, developing as a disseminated disease infiltrating lymph nodes (LN) and bone marrow (BM)[1]. Within invaded LN, malignant germinal center (GC)-derived B cells are found admixed with various non-neoplastic cells including follicular helper $CD4^+$ T cells (Tfh), lymphoid stromal cells, and macrophages, organized in follicular structures mirroring normal GC[2,3]. Indeed, FL is considered as a B-cell malignancy strongly dependent on a GC-like permissive microenvironment exhibiting FL-specific features. FL-infiltrating lymphoid stromal cells have recently emerged as key drivers of FL-supportive niche. In agreement, the commitment of mesenchymal progenitors towards lymphoid-like stromal cell differentiation *in vitro*, through a combination of tumour necrosis factor-α (TNF) and lymphotoxin-$\alpha 1\beta 2$ (LT), is associated with an increased capacity to sustain FL B-cell survival[4]. Moreover, FL stromal cells were shown to overexpress CXCL12 *in situ*, contributing to migration, adhesion, and activation of FL B cells[5]. Such specific alteration is associated with an extensive remodeling of LN stromal cell phenotype[5–7].

Besides nodal sites, BM infiltration is found in 40-70% of FL patients at diagnosis, preferentially with paratrabecular focal localizations, and is an important adverse factor in FL clinical risk-stratification scores[8–10]. Interestingly, BM FL B cells are characterised by a lower cytological grade, a decreased proliferation, and a modified phenotype with reduced CD10 expression compared with LN FL B cells[11]. Moreover, somatic hypermutation analysis and targeted deep sequencing have demonstrated that different FL B-cell subclones could be detected within LN *versus* BM, and suggested that FL originates in the LN and infiltrates BM early in the course of the disease, allowing further accumulation of BM-specific mutations[11–13]. How tumor B cells are engaged in a bidirectional crosstalk with the BM microenvironment and what are the specific features of BM FL B cells remain largely unknown. Mesenchymal stromal cells (MSC) obtained from FL BM display a specific gene expression profile (GEP), including an enrichment for a lymphoid-stromal cell signature, and an increased capacity to sustain FL B-cell growth compared to BM-MSC obtained from healthy donors (HD)[14]. In addition, CXCL12 is specifically induced in BM-MSC infiltrating FL BM aggregates[5]. Finally, FL BM-MSC also contribute to the organization of FL niche by recruiting protumoral monocytes and neutrophils through CCL2 and IL8, respectively[14,15]. Both IL-8 and CCL2 could be increased in HD BM-

MSC by the contact with FL B cells, suggesting that a dynamic reciprocal cooperation program is activated between FL B cells and FL infiltrating stromal cells[14,15]. Importantly, the early driver mechanism triggering the formation of this medullar FL permissive niche has not been yet identified.

Extracellular vesicles (EVs) are heterogeneous lipid bilayer-enclosed particles released from normal and malignant cells, involved in cell-cell communication by transferring their bioactive cargos to recipient cells, and playing key roles in cancer biology[16]. Recent studies have demonstrated that EVs released by cancer cells could be incorporated by BM-MSC and contribute to their reprogramming into tumor-supportive cancer-associated fibroblasts (CAF). This is in particular the case in lymphoid malignancies developing within the BM, such as multiple myeloma and chronic lymphocytic leukemia[17–21]. However, no data are currently available regarding the role and properties of EVs in FL. In the current work, we report that FL B cells produce EVs that can be internalized by BM-MSC, making them more efficient to support FL B-cell survival. Moreover, this supportive phenotype is different from the one obtained under TNF/LT stimulation, in agreement with the engagement of different signalling pathways in BM-MSC and includes a strong upregulation of genes previously involved in the hematopoietic stem cell (HSC) niche. Finally, BM-MSC priming by FL-derived EVs promote FL B cells with a quiescent phenotype mimicking those of BM FL B cells. Altogether these data support a role of EVs in FL dissemination and drug resistance.

PATIENTS, MATERIALS, AND METHODS

Patients and samples

The research protocol was conducted under French legal guidelines with informed consent and was approved by the local ethics committee. LN and BM aspirates were obtained from patients with FL at diagnosis and BM were also collected from age-matched patients undergoing cardiac surgery. BM plasma were collected by centrifugation and frozen at -80°C until use. Ex vivo-expanded BM-MSC and LN-derived lymphoid stromal cells (LSC) were obtained as previously described[4,14,22]. The GEP of BM-MSC and LN-LSC was studied at the end of passage 1, and BM-MSC were used at passages 2 to 3 for functional studies. For functional studies, HD B cells from tonsil and primary FL B cells from LN were purified using the B-cell isolation kit II (Miltenyi Biotec). Purified LN FL B cells were also used to stimulate

BM-MSC for 3 days as previously described[4] before sorting of $CD45^{neg}CD105^{pos}$ BM-MSC for GEP. For malignant B-cell GEP, $CD20^{hi}CD44^{lo}$ $CD38^{pos}IgD^{neg}CD138^{neg}CD34^{neg}$ viable FL B cells were sorted from LN and invaded BM using a FACSAria (BD Biosciences). GC-derived lymphoma B-cell lines RL, SUDHL4, and DOHH2 were obtained from the DSMZ and were maintained in RPMI1640 supplemented with 7% fetal calf serum (FCS, Gibco) depleted from residual EVs by filtering at 200 nm followed by a 16-hour ultracentrifugation at 100,000 g.

EV purification

All the experiments related to EV purification and characterization were performed according to the *Minimal information for the studies of extracellular vesicles* guideline of the International Society for Extracellular Vesicles[23] and were detailed in the Supplemental Methods.

Study of BM-MSC priming by EVs

Analysis of the impact of EVs on BM-MSC RNAseq and function and study of the underlying signaling pathways were detailed in the Supplemental Methods.

GEP analysis of Affymetrix microarrays

RNA was extracted from 8 FL BM-MSC, 8 FL LN-LSC, 6 HD BM-MSC primed or not by primary FL B cells, 5 BM FL B cells, and 10 LN FL B cells using Qiazol lysis with DNAse treatment (Qiagen) and RNA purity and integrity checked using the Bioanalyzer 2100 before analysis on GeneChip HG-U133 Plus 2.0 oligonucleotide microarrays (Affymetrix). In addition, we reanalyzed the GEP of our previous cohort of 10 FL BM-MSC, including 6 coming from histologically invaded BM and 4 from histologically non-invaded BM, compared with 6 age-matched HD BM-MSC[14].

Analysis of differentially expressed genes, Weighted Gene Correlation network analysis (WGCNA), biological pathway enrichment analysis, and analysis of the similarities between BM-MSC GEP and mouse scRNAseq data were described in Supplemental Methods together with the validation of differentially expressed genes by qPCR.

Cytokine quantification

ANGPT1, TGFB1 (R&D Systems), and CXCL12 (Merck Millipore) were quantified on BM plasma by Luminex technology.

Analysis of the interactome between FL B cells and stromal cells

Interactome analysis was performed with the NicheNet ligand activity algorithm[24] in order to investigate the interface between EV-primed BM-MSC and BM FL-B cells, and between TNF/LT-primed BM-MSC and LN FL B cells. For details, see online Supplemental Methods.

Statistics

Statistical test and graphic representation of the TRPS, cytometry, qPCR and Luminex data were performed with Prism software version 5 (GraphPad Software). Statistical significance was determined using ANOVA, nonparametric Wilcoxon test for matched pairs, or Mann- Whitney nonparametric U test as appropriate. Data were presented as the mean +/- standard deviation or as the median depending on the statistical test used.

Data sharing: Data are available under Dataset 1 -> GSE152386 Dataset 2 -> GSE152386 & GSE152068 Dataset 3 -> GSE35331 Dataset 4 -> GSE152215 & GSE85233 & GSE136249

s

RESULTS

FL-derived EVs are internalized by BM-MSC

Accumulating evidence suggests that EVs are an important mechanism underlying the intercellular communications within malignant cells and their microenvironment. We thus purified EVs from conditioned media of FL B-cell lines and primary FL B cells using serial ultracentrifugation. EV size and concentration were studied and ranged from 60 nm to 300 nm with a mode of 90-110 nm, and from 4 x 10^8 to 2.3 x 10^{10} particles/10^4 malignant B cells (Figures 1 A-C). We further validated that purified FL-derived vesicles expressed conventional EV markers, including the endosome-associated protein TSG101 and the tetraspanin CD81, in the absence of the contamination markers Golgin and Calnexin (Supplemental Figure 1). Importantly,

confocal microscopy and flow cytometry experiments revealed that BM-MSC efficiently uptaked dyed EVs derived from FL B cells (Supplemental Figure 2), whereas no transfer was observed on incubation at 4°C (Figures 1D). In addition, the use of endocytosis inhibitors, including EDTA, sucrose and cytochalasin, and the specific targeting of the clathrin- and caveolin-dependent pathways through the dynamin-2 inhibitor Dynasore strongly reduced incorporation of FL-derived EVs in BM-MSC (Figure 1D). We previously demonstrated that BM-MSC could support FL B-cell survival *in vitro*[4,14]. To evaluate how FL-derived EVs could modify the tumor-supportive capacity of BM-MSC, we performed coculture experiments using purified primary FL B cells. As expected, HD BM-MSC efficiently sustained the survival of neoplastic B cells. Moreover, preliminary treatment by FL-derived EVs significantly reinforced this feeder effect ($P < .01$; Figure 1E). Altogether, these data demonstrate that FL-derived EVs trigger BM-MSC towards a FL-supportive phenotype.

FL-derived EVs and TNF/LT differentially prime BM-MSC towards a FL stroma-like phenotype

The priming of HD BM-MSC by TNF/LT was shown to trigger a FL-supportive phenotype and FL BM-MSC have been described as ectopically committed towards lymphoid stroma differentiation[4,14]. We thus decided to compare the GEP of 5 HD BM-MSC stimulated by FL-derived EVs (obtained from 3 different FL B-cell lines) or TNF/LT, looking for molecular similarities and differences between these two types of induced tumor-promoting stroma. RNAseq analysis revealed a lack of significant overlap between the signatures induced by EVs *versus* TNF/LT ($P = 1$, hypergeometric test; Figure 2A), delineating a specific EV signature (1218 upregulated genes) and a specific TNF/LT signature (1312 upregulated genes) (Supplemental Table S2). In order to evaluate the biological relevance of these two signatures, we then tested whether they were enriched in FL-infiltrating stromal cells obtained from BM (FL BM-MSC) or LN (FL LN lymphoid stromal cells, FL LN-LSC). For that purpose, we examined the GEP of FL BM-MSC (n=8) and FL LN-LSC (n=8) using Affymetrix microarrays. Unsupervised principal component analysis (PCA) performed on all expressed genes adequately segregated the two FL stromal cell subsets (Figure 2B) and we identified 1050 genes specifically upregulated in FL BM-MSC and 874 genes specifically upregulated in FL LN-LSC (Supplemental Table S3). Interestingly, GSEA revealed that whereas the TNF/LT signature was enriched in FL

LN-LSC, in agreement with their localization within heavily infiltrated lymphoid tissues, FL BM-MSC transcriptomic profile was strongly enriched for the EV signature, raising the hypothesis that FL-derived EVs could contribute to the activation of stromal cells outside the primary LN niches (Figure 2C). To extend these data we took the opportunity of reanalyzing our previous GEP cohort of 10 FL BM-MSC, including 6 coming from histologically invaded BM and 4 from histologically non-invaded BM, compared with 6 age-matched HD BM-MSC[14]. First, a PCA performed on the 2389 genes differentially expressed between FL BM-MSC and HD BM-MSC (FDR<1%) suggested that BM-MSC obtained from invaded BM could be distinguished from those obtained from non-invaded BM (Supplemental Figure 3A). Moreover, the TNF/LT signature, unlike the EV signature, was enriched in BM-MSC in close contact with FL B cells within invaded BM, confirming that the TNF/LT signature, unlike the EV signature, was related to direct contact of BM-MSC with malignant B cells (Supplemental Figure 3B). To further understand the direct impact of malignant B cells on BM-MSC phenotype, we performed 3-day cocultures (n=6) of purified primary FL B cells with HD BM-MSC and analyzed the GEP of cell-sorted primed BM-MSC (Supplemental Table S4). Importantly, GSEA highlighted that this 1716-gene signature was significantly enriched in FL BM-MSC compared to HD BM-MSC, thus validating the relevance of our *in vitro* approach (Supplemental Figure 3C). To decipher the relationship between the BM-MSC phenotype induced by FL-derived EV versus FL B cells we then delineated the specific FL B-cell primed signature (1551 upregulated genes, Supplemental Figure 3D). Interestingly, whereas this signature was not enriched in FL BM-MSC versus FL LN-LSC, it was strongly enriched in BM-MSC obtained from invaded *versus* non-invaded BM (Supplemental Figure 3E-F), further suggesting a role of EVs in the activation of BM-MSC before BM seeding by malignant B cells.

To explore the EV signature more deeply, we next submitted it to pathway enrichment analysis using Gene Ontology (GO), REACTOME, and MSigDB databases (Figure 2D-E and Supplemental Table S5). Whereas the TNF/LT signature was associated to inflammation- and NF-κB-related pathways (Supplemental Figure 4 and Supplemental Table S5), the EV signature was enriched for cell signaling and cell communication biological processes, cytokine/chemokine signaling, including IL-6, IL-7, and TGF-β, and pathways related to bone and cartilage development. This result prompted us to compare our data to the recently

published mouse datasets describing the heterogeneity of steady state BM-MSC[25,26]. Interestingly, BM-MSC stimulated by FL-derived EVs harbored a GEP close to that of Leptin receptor (Lepr)^{pos} MSC and MSC-derived early osteolineage cells (OLC), both reported to be key cell subsets of HSC niche (Figure 2F). Conversely, the signature of TNF/LT primed BM-MSC did not match to a specific mouse BM stromal cell subset. Altogether, these data demonstrate that FL-derived EVs trigger a particular phenotype in HD BM-MSC, sharing features with FL-infiltrating stromal cells and HSC stromal niche.

BM-MSC stimulated by FL-derived EVs upregulated genes of HSC and FL BM niche

Detailed analysis of EV-primed BM-MSC signature highlighted all the master genes involved in HSC maintenance and regulation. In particular, *CXCL12*, *Angiopoietin-1 (ANGPT1)* and *-2 (ANGPT2*), *KITLG/SCF, and EPHB4* were upregulated by FL-derived EVs, similarly to *IL7*, a key factor of early commitment towards B-cell lineage, recently shown to be co-expressed in perisinusoidal cells with CXCL12 and KITLG/SCF[27] (Figure 3A). Apart from these functional markers, FL-derived EVs did not trigger the classical markers of MSC compartment, such as *LEPR*, *NES*, *NG2*, or *CD200*[26], but upregulated markers of osteolineage differentiation including *RUNX2*, the master regulator transcription factor controlling the commitment of MSC to OLC[28], and *SP7*, its downstream target. The lack of induction of mature OLC markers, including *BGLAP*, *ALPL*, or *SPP1*, argued for an osteo-primed MSC stage rather than a full osteoblastic differentiation. In agreement, repeated stimulation of HD BM-MSC with FL-derived EVs triggered partial osteoblastic differentiation compared to that obtained with classical osteoblastic differentiation medium (Supplemental Figure 5). Moreover, the adipogenic marker *PPARG* was also upregulated in response to stimulation by FL-derived EVs, generating a phenotype close to that of the Lepr^{+} cells of HSC niche that coexpress a unique combination of adipogenic and osteogenic transcription factors[29]. Finally, both *FOXC1* and *EBF1*, the two transcription factors essential for the formation and maintenance of HSC niche and for the inhibition of full adipocyte and osteoblast differentiation[30,31], were upregulated by FL-derived EVs in BM-MSC. Collectively, EVs-primed BM-MSC expressed the specific panel of transcription factors, cytokines, and chemokines previously reported in HSC stromal cell niches. Of note, *RUNX2* and *EPHB4* were both also upregulated by priming of BM-MSC with primary FL B cells (Supplemental Figure 3D). Conversely, the TNF/LT-

induced signatures associated with a decreased expression of *CXCL12, ANGPT2*, and *RUNX2* together with an upregulation of inflammatory cytokines, including *IL1A, IL1B, IL6, IL15*, inflammatory chemokines, such as *CCL2, CXCL8, CXCL10, CX3CL1*, and adhesion molecules *ICAM1, VCAM1*, and *ITGAV* (Figure 3A). Of note, TGF-β signaling has been identified as regulating HSC quiescence in BM niche and both *TGFB1* and *TGFB3* were significantly upregulated in EV-primed *versus* TNF/LT-primed BM-MSC. All these data were confirmed by qPCR in BM-MSC treated by TNF/LT (n=9) *versus* FL-derived EVs (n=27) (Figure 3B).

To evaluate the relevance of these observations for FL BM niche, we stimulated BM-MSC with EVs isolated from BM plasma of FL patients (n=13) *versus* age-matched HD (n=6) and characterized by transmission electron microscopy and tunable resistive pulse sensing (TRPS) (Figure 4A-B). Interestingly, the hematopoietic cytokines *CXCL12, ANGPT1, TGFB3*, and *IL7*, as well as the master regulators of HSC niche formation *EBF1* and *FOXC1* were significantly induced by EVs obtained from FL BM compared to HD BM, suggesting that the polarization process observed *in vitro* could take place within FL BM niches (Figure 4C). In addition, whereas the level of IL-7 and TGF-β3 remained below the quantification level in all BM plasma tested, we could extend our previous demonstration of CXCL12 upregulation within FL BM niche[5] and identified a significant increase of Angiopoietin-1 and TGF-β1 levels in FL BM plasma (Figure 4D).

FL-derived EVs activated various signaling pathways in BM-MSC

We next try to identify the signaling pathways activated by FL-derived EVs in BM-MSC. For that purpose, we first evaluated the enrichment for transcription factor motifs in the promoters of genes upregulated in EV versus TNF/LT signatures and the enrichment for transcription factor targets in these two signatures (Figure 5A-B). TNF/LT signature was in particular associated with NF-κB and IRF signaling pathways whereas EV signature revealed activity of SOXs, SMADs, MTA1, or EZH2 transcription factors, all previously reported in the TGF-β signaling pathway[32]. Interestingly, besides numerous proteins related to B-cell activation, including BTK, CD81, CD79A, MME, or MHC class II, quantitative proteomics of EVs by liquid chromatography-mass spectrometry (LC-MS/MS) revealed the presence of higher levels of TGF-β1 in FL B-cell derived EVs compared to tonsil B-cell derived EVs

(Supplemental Table S6). In agreement, FL-derived EVs did not trigger the nuclear translocation of NF-κB p65 subunit in HD BM-MSC (Supplemental Figure 6A) but induced activation of SMAD2/3-SMAD4 in a TGF-β sensor cell line (Figure 5C). Of note, SMAD activation by FL-derived EVs was specifically reversed by the TGFBR1 inhibitor Galunisertib and was not induced by tonsil B-cell derived EVs, in agreement with the upregulation of *TGFB1* recently reported in primary purified FL B cells compared to normal GC B cells[33]. Finally, FL-derived EVs activated SMAD2/3 and p38 pathways, related to canonical and non-canonical TGF-β signaling, in BM-MSC (Figure 5D). Importantly, Galunisertib inhibited only partly the activity of FL-derived EVs as highlighted by the reduction of *RUNX2* and *EPHB4* but not *ANGPT1* expression (Figure 5E). This could be related to the fact that FL-derived EVs also triggered non-TGFβ related signaling pathways, including activation of STAT6, unlike STAT1/3/5, phosphorylation (Supplemental Figure 6B). STAT6 was also identified within the proteins enriched in FL-derived EVs compared to tonsil B-cell derived EVs (Supplemental Table S6) reinforcing the hypothesis of STAT6 triggering in BM-MSC by FL-derived EVs. Altogether, these data suggest that FL-derived EVs activated TGF-β dependent and TGF-β independent activation pathways in BM-MSC, that are essentially not triggered by tonsil-derived EVs as confirmed at the transcriptomic level (Figure 5F).

BM FL B cells specifically interact with BM-MSC primed by FL-derived EVs

Having demonstrated that LN and BM stromal cells from FL patients displayed different GEP, enriched for TNF/LT *versus* EVs signatures respectively, we wondered whether FL B cells purified from LN *versus* BM also exhibited specific molecular features. For that purpose, we analyzed the transcriptome of sorted $CD20^{hi}CD44^{lo}CD38^{pos}IgD^{neg}CD138^{neg}CD34^{neg}$ B cells obtained from invaded LN (n=10) and BM (n=5). The first parameter impacting FL B-cell GEP was the inter-individual variability, as highlighted by the close relationship between autologous LN and BM B cells in unsupervised Pearson correlation (Figure 6A). We then applied an unsupervised WGCNA to identify transcriptional modules of co-expressed genes and evaluate whether they were related to FL B-cell origin. The coexpression network constructed by using the WGCNA algorithm allowed us to identify 17 distinct gene modules (Supplemental Figure 7A). We then determined whether the module

eigengenes were significantly different in BM *versus* LN FL B cells (Supplemental Figure 7B). Two modules (Blue_module 1 and Brown_module 2) were significantly associated with the FL B-cell origin and the top 10 GO terms associated with both of them highlighted a downregulation of genes involved in cell cycle and fatty acid metabolism in BM FL B cells, indicating that interacting with a different microenvironment impacted FL B cell profile (Figure 6B). We next identified the 595 differentially expressed genes between LN and BM FL B cells and revealed by GSEA that BM FL B cell GEP reflected a reduced proliferation and active metabolism (Figure 6C-D). In agreement, BM FL B cells overexpressed the antiproliferative genes *BTG1*, previously involved in T-cell and HSC quiescence[34,35], *CKAP4*, and *LZTS3*[36], but also *Dysadherin/FXYD5*, a molecule involved in drug resistance and cell motility in cancer stem cells[37] (Supplemental Table S7). Finally, we confirmed by qPCR the lower expression of *MKI67* and *CDK1* in BM FL B cells *versus* LN FL B cells (Figure 6E).

Given the specific similarities between EV-primed BM-MSC and BM FL stroma, we then evaluated the impact of EV-primed BM-MSC on primary FL B cells purified from invaded LN, compared to TNF/LT-primed BM-MSC as a reference of lymphoid-committed stromal cells (Figure 7A). Interestingly, FL B cells cocultured with EV-primed BM-MSC exhibited a decreased expression of CD86 and a lower rate of proliferation, without difference in cell survival compared to coculture with TNF/LT-derived BM-MSC (data not shown). Finally, based on our two FL-supportive stromal cell signatures and on the list of genes upregulated in BM and LN FL B cells compared to normal centrocytes[38] (Supplemental Table S8), we next applied the new computational method NicheNet[24] to delineate the specific interactions underlying the crosstalk between FL B cells and stromal cells, defining stromal cells as sender cells and B cells as receiver cells (Figure 7B). Using this strategy, we highlighted, as expected, CXCL12, and TGFB3 at the specific interface between BM FL B cells and EV-primed BM-MSC and we also identified several members of the Eph/ephrin receptor family known to mediate cell-cell signals in a variety of physiological contexts. Conversely, the crosstalk between LN FL B cells and TNF/LT-primed BM-MSC specifically involved IL-6, IL-15, and TNFSF13B/BAFF pathways.

DISCUSSION

FL is characterized by a frequent BM infiltration by malignant B cells displaying BM-specific phenotypic and genetic features, associated with an alteration of the local immune and stromal microenvironment, supporting a key role for bidirectional interactions between FL cells and their surrounding medullar niche[39–41]. The specific gene signature of FL BM stromal cells was initially identified as independent of the infiltration extend[14], suggesting additional mechanisms of stroma polarization besides direct cell-cell contact. Several reports have demonstrated that EVs released by malignant cells from primary solid tumors can modify distal sites, including the BM, to promote metastasis[42,43]. In the current study, we thus explored the relationship between FL BM stroma and FL BM B-cell features and how FL-derived EVs could contribute to the commitment of BM-MSC towards a lymphoma-supportive stroma.

We first demonstrated that FL-derived EVs strongly modified the GEP of BM-MSC, triggering an upregulation of HSC niche factors, including CXCL12. Such induction of CXCL12 in the BM stroma by tumor EVs has been recently described in prostate cancers and was shown to be dependent on the upregulation of HIF-1α[43], which is also induced in BM-MSC by FL-derived EVs (Supplemental Table S2). CXCL12 supports FL B cell migration, adhesion, and survival[5], and could thus be involved in the homing and growth of BM FL B cells. Of note FL-derived EVs also triggered angiopoetin-1 in BM-MSC and we confirmed its increased amount in FL BM plasma. In the context of myeloid neoplasms tumor-EVs repress angiopoietin-1 expression[44], demonstrating that supportive stroma phenotypes are tumor-specific. Collectively, the aberrant expression of hematopoietic niche factors in FL BM could contribute to the deregulated hematopoiesis described in patients with mature B-cell malignancies even in the absence of detectable BM involvement[45]. Importantly, EVs could also have an impact on the immune compartments of tumor microenvironment. In particular, tumor-derived EVs have been involved in the polarization of tumor-associated macrophages (TAM) in Waldenstrom macroglubulinemia[46], and diffuse large B-cell lymphomas (DLBCL), the most frequent aggressive B-cell lymphoma, in which EV-primed macrophages were shown to sustain malignant B-cell proliferation and migration[47]. Given the key role of TAM in FL pathogenesis it would be interesting to evaluate how FL-derived EVs contribute to their reprogramming. Finally, we cannot exclude that tumor EVs could directly favor malignant B-cell growth through the delivery of FL B-cell growth factors, as suggested for the activity of IL-31[48].

EVs from Hodgkin lymphomas promote a proinflammatory and proangiogenic NF-κB-dependent phenotype in fibroblasts[49]. Conversely, stroma reprogramming by FL-derived EVs seems to be NF-kB independent and is not associated with activation of inflammatory pathways. However, malignant FL B cells could also directly affect the phenotype and function of infiltrating stromal cells, and the release of TNF/LT by tumor B cells has been involved in the upregulation of CCL2 and IL-8 in BM and LN FL stroma[14,15]. The net effect of EVs *versus* direct contact with tumor cells on the phenotype of FL stromal cells probably depend on both the tumor site, *i.e.* primary LN *versus* distant BM, and the kinetic of lymphoma evolution, with an increase of BM involvement in more advanced stage of the disease. Of note, when BM-MSC were treated by a combination of TNF/LT and FL-derived EVs, CXCL12 was downregulated indicating a dominant effect of the contact with B cells (data not shown), thus explaining the discrepancy between BM and LN stroma phenotypes. Besides malignant B cells, FL tumor microenvironment could contribute to FL stroma polarization. This is in particular the case for FL-infiltrating Tfh that overexpress IL-4 and promote CXCL12 expression in FL LN stromal cells[5]. Interestingly, stimulation of BM-MSC by FL-derived EVs induced an upregulation of *IL4R*, *STAT6*, and *CD40* (Supplemental Figure S8) all involved in the response to IL-4- and CD40L-expressing T cells, and FL-derived EVs were enriched for STAT6 protein. Importantly, very few T cells with a full Tfh phenotype could be detected in FL BM and CD4/CD8 ratio was found increased only in heavily involved BM, whereas the level of CXCL12 is already increased in non-involved BM plasma. These data suggested that EVs could contribute to CXCL12 upregulation in the absence of direct contact with malignant B cells, but could then synergize with IL-4 produced by infiltrating T cells admixed with FL B cells[5].

EVs are known to trigger complex signaling networks in CAF, related to the delivery of numerous proteins, RNA, and lipids. Interestingly, we highlighted a TGF-β dependent activation of BM-MSC by FL-derived EVs. Expression of TGF-β by LN FL B cells has been previously described and was involved in the alteration of intratumoral T-cell function[50,51]. More recently, an integrative analysis of FL cell niche revealed enrichment for gene networks related to TGF-β signaling[33]. How TGF-β and STAT6 pathways could synergize for the acquisition of FL CAF phenotype remains to be explored. These data, together with our current demonstration that FL-derived

EVs could contribute to the TGF-β dependent activation of distant BM-MSC, support TGF-β as a putative target deserving further investigations.

FL BM-MSC support malignant B cells with a lower proliferation rate than LN FL B cells[10]. In the current study we provide the first characterization of BM FL B cell GEP and confirmed their quiescent phenotype, associated with the upregulation of the antiproliferative gene *BTG1*. Interestingly, a $BTG1^{hi}$ phenotype was recently associated with a good prognosis in aggressive DLBCL[52], in association with a decreased cell cycle, confirming a role for BTG1 in the regulation of cell proliferation in GC-derived B-cell lymphomas. The analysis of the interactome between BM FL B cells and EVs-primed BM-MSC highlights not only CXCL12 but also Eph/ephrin pathway. Silencing EphA7 receptor, a decoy receptor blocking Eph signaling, has been shown to drive lymphoma development in a murine FL model[53], suggesting that ephrin-dependent activation could have a protumoral activity in FL.

Our study suggests that FL-derived EVs should be considered as putative mediators of BM stroma polarization. Moreover, EVs released by lymphoma B cells were already demonstrated to bound therapeutic anti-CD20 antibodies, protecting malignant cells from antibody attack[54]. In this context, the blockade of EV release was proposed as clinically relevant to restore sensitivity to immunotherapy. Whether FL pathogenesis might be also influenced by EVs released by the tumor microenvironment, as previously reported for other hematopoietic malignancies[55], remains to be elucidated. Besides the mechanism of BM stroma reprogramming, BM forms a survival niche supporting resistance to treatment and inducing LN relapses[12] in FL, supporting the clinical interest of targeting the crosstalk between BM-MSC and malignant B cells, either through the inhibition of stroma-derived B-cell growth factors or through the mobilization of FL B cells outside their supportive BM niche.

ACKNOWLEDGMENTS

This work was supported by research grants from Fondation ARC (PGA1 RF20170205386), the Institut National du cancer (INCA AAP PNP19-009) and the Infrastructure program EcellFRANCE (ANR-11-INSB-005) and was part of the "Carte d'Identité des Tumeurs (CIT)" program developed by the Ligue contre le Cancer. SL is supported by the chair "Cancer & Innovation" of Rennes 1 Foundation. We thank the personnel of CIT platforms for RNA qualification (Saint-Louis Hospital, Paris) and Affymetrix expression arrays (Institut de Génétique et de Biologie Moléculaire et Cellulaire, Strasbourg). RNAseq has been performed by the ICGex NGS platform of the Institut Curie supported by the grants ANR-10-EQPX-03 (Equipex) and ANR-10-INBS-09-08 (France Génomique Consortium) from the Agence Nationale de la Recherche ("Investissements d'Avenir" program), by the ITMO-CANCER and by the SiRIC-Curie program - SiRIC Grant « INCa-DGOS- 4654 ». Proteomic studies were supported by "Région Ile-de-France" and Fondation pour la Recherche Médicale grants to DL. Some bone marrow plasma were obtained from patients included in the BIO-FLIRT study as a part of the ancillary study of the FLIRT trial (NCT02303119) sponsored by the Lymphoma Academic Research Organisation (LYSA). T Immunofluorescence study was performed on the Microscopy Rennes Imaging Center (MRic-ALMF; UMS 6480 Biosit, Rennes, France). Transmission Electron Microscopy was realized in the same platform microscopy center in collaboration with Agnes Burel. The authors are indebted to the Centre de Ressources Biologiques (CRB)-Santé (BB-0033-00056, http://www.crbsante-rennes.com) of Rennes hospital for its support in the processing of biological samples.

AUTHORSHIP CONTRIBUTIONS

ED: designed and performed experiments, analyzed data, and wrote the paper; CP: provided data on FL B cell gene expression profile; DR, SL: contributed to data analysis; MD, CC: provided the SMAD2/3-SMAD4 reporter cell line, TM: contributed to study design; ML, JD: provided technical assistance; PL: run RNA sequencing; FD: carried out the MS experimental work, DL: supervised MS experiments and data analysis; EF, GC: provided samples, TF: provided samples and contributed to study design; KT: designed and supervised research, and wrote the paper.

CONFLICT-OF-INTEREST DISCLOSURE

This study has used some samples collected owing to the Bio-FLIRT funding as a part of the ancillary FLIRT study. The authors declare no other competing financial interest.

REFERENCES

1. Huet S, Sujobert P, Salles G. From genetics to the clinic: a translational perspective on follicular lymphoma. *Nature Reviews Cancer*. 2018;18(4):224–239.
2. Lamaison C, Tarte K. Impact of B cell/lymphoid stromal cell crosstalk in B-cell physiology and malignancy. *Immunology Letters*. 2019;215:12–18.
3. Amé-Thomas P, Tarte K. The yin and the yang of follicular lymphoma cell niches: role of microenvironment heterogeneity and plasticity. *Semin. Cancer Biol.* 2014;24:23–32.
4. Amé-Thomas P, Maby-El Hajjami H, Monvoisin C, et al. Human mesenchymal stem cells isolated from bone marrow and lymphoid organs support tumor B-cell growth: role of stromal cells in follicular lymphoma pathogenesis. *Blood*. 2007;109(2):693–702.
5. Pandey S, Mourcin F, Marchand T, et al. IL-4/CXCL12 loop is a key regulator of lymphoid stroma function in follicular lymphoma. *Blood*. 2017;129(18):2507–2518.
6. Chang K-C, Huang X, Medeiros LJ, Jones D. Germinal centre-like versus undifferentiated stromal immunophenotypes in follicular lymphoma. *The Journal of Pathology*. 2003;201(3):404–412.
7. Pepe G, Napoli AD, Cippitelli C, et al. Reduced lymphotoxin-beta production by tumour cells is associated with loss of follicular dendritic cell phenotype and diffuse growth in follicular lymphoma. *The Journal of Pathology: Clinical Research*. 2018;4(2):124–134.
8. Solal-Céligny P, Roy P, Colombat P, et al. Follicular Lymphoma International Prognostic Index. *Blood*. 2004;104(5):1258–1265.
9. Federico M, Bellei M, Marcheselli L, et al. Follicular Lymphoma International Prognostic Index 2: A New Prognostic Index for Follicular Lymphoma Developed by the International Follicular Lymphoma Prognostic Factor Project. *JCO*. 2009;27(27):4555–4562.
10. Bachy E, Maurer MJ, Habermann TM, et al. A simplified scoring system in de novo follicular lymphoma treated initially with immunochemotherapy. *Blood*. 2018;132(1):49–58.
11. Bognár Á, Csernus B, Bödör C, et al. Clonal selection in the bone marrow involvement of follicular lymphoma. *Leukemia*. 2005;19(9):1656–1662.
12. Wartenberg M, Vasil P, zum Bueschenfelde CM, et al. Somatic hypermutation analysis in follicular lymphoma provides evidence suggesting bidirectional cell migration between lymph node and bone marrow during disease progression and relapse. *Haematologica*. 2013;98(9):1433–1441.
13. Araf S, Wang J, Korfi K, et al. Genomic profiling reveals spatial intra-tumor heterogeneity in follicular lymphoma. *Leukemia*. 2018;32(5):1261–1265.
14. Guilloton F, Caron G, Ménard C, et al. Mesenchymal stromal cells orchestrate follicular lymphoma cell niche through the CCL2-dependent recruitment and polarization of monocytes. *Blood*. 2012;119(11):2556–2567.
15. Grégoire M, Guilloton F, Pangault C, et al. Neutrophils trigger a NF-κB dependent polarization of tumor-supportive stromal cells in germinal center B-cell lymphomas. *Oncotarget*. 2015;6(18):16471–16487.
16. Kalluri R, LeBleu VS. The biology, function, and biomedical applications of exosomes. *Science*. 2020;367(6478).

17. Longjohn MN, Hudson J-ABJ, Smith NC, et al. Deciphering the messages carried by extracellular vesicles in hematological malignancies. *Blood Reviews*. 2020;100734.
18. Dubois N, Crompot E, Meuleman N, et al. Importance of Crosstalk Between Chronic Lymphocytic Leukemia Cells and the Stromal Microenvironment: Direct Contact, Soluble Factors, and Extracellular Vesicles. *Front Oncol*. 2020;10:1422.
19. Ghosh AK, Secreto CR, Knox TR, et al. Circulating microvesicles in B-cell chronic lymphocytic leukemia can stimulate marrow stromal cells: implications for disease progression. *Blood*. 2010;115(9):1755–1764.
20. Farahani M, Rubbi C, Liu L, Slupsky JR, Kalakonda N. CLL Exosomes Modulate the Transcriptome and Behaviour of Recipient Stromal Cells and Are Selectively Enriched in miR-202-3p. *PLOS ONE*. 2015;10(10):e0141429.
21. Paggetti J, Haderk F, Seiffert M, et al. Exosomes released by chronic lymphocytic leukemia cells induce the transition of stromal cells into cancer-associated fibroblasts. *Blood*. 2015;126(9):1106–1117.
22. Gallouet A-S, Travert M, Bresson-Bepoldin L, et al. COX-2–Independent Effects of Celecoxib Sensitize Lymphoma B Cells to TRAIL-Mediated Apoptosis. *Clin Cancer Res*. 2014;20(10):2663–2673.
23. Théry C, Witwer KW, Aikawa E, et al. Minimal information for studies of extracellular vesicles 2018 (MISEV2018): a position statement of the International Society for Extracellular Vesicles and update of the MISEV2014 guidelines. *Journal of Extracellular Vesicles*. 2018;7(1):1535750.
24. Browaeys R, Saelens W, Saeys Y. NicheNet: modeling intercellular communication by linking ligands to target genes. *Nature Methods*. 2020;17(2):159–162.
25. Tikhonova AN, Dolgalev I, Hu H, et al. The bone marrow microenvironment at single-cell resolution. *Nature*. 2019;569(7755):222.
26. Baryawno N, Przybylski D, Kowalczyk MS, et al. A Cellular Taxonomy of the Bone Marrow Stroma in Homeostasis and Leukemia. *Cell*. 2019;177(7):1915-1932.e16.
27. Balzano M, De Grandis M, Vu Manh T-P, et al. Nidogen-1 Contributes to the Interaction Network Involved in Pro-B Cell Retention in the Peri-sinusoidal Hematopoietic Stem Cell Niche. *Cell Reports*. 2019;26(12):3257-3271.e8.
28. Huang W, Yang S, Shao J, Li Y-P. Signaling and transcriptional regulation in osteoblast commitment and differentiation. *Front. Biosci.* 2007;12:3068–3092.
29. Omatsu Y, Sugiyama T, Kohara H, et al. The Essential Functions of Adipo-osteogenic Progenitors as the Hematopoietic Stem and Progenitor Cell Niche. *Immunity*. 2010;33(3):387–399.
30. Omatsu Y, Seike M, Sugiyama T, Kume T, Nagasawa T. Foxc1 is a critical regulator of haematopoietic stem/progenitor cell niche formation. *Nature*. 2014;508(7497):536–540.
31. Seike M, Omatsu Y, Watanabe H, Kondoh G, Nagasawa T. Stem cell niche-specific Ebf3 maintains the bone marrow cavity. *Genes Dev.* 2018;32(5–6):359–372.
32. Li L, Liu J, Xue H, et al. A TGF-β-MTA1-SOX4-EZH2 signaling axis drives epithelial-mesenchymal transition in tumor metastasis. *Oncogene*. 2020;39(10):2125–2139.
33. Pangault C, Amé-Thomas P, Rossille D, et al. Integrative Analysis of Cell Crosstalk within Follicular Lymphoma Cell Niche: Towards a Definition of the FL Supportive Synapse. *Cancers*. 2020;12(10):2865.

34. Yuniati L, Scheijen B, van der Meer LT, van Leeuwen FN. Tumor suppressors BTG1 and BTG2: Beyond growth control. *J. Cell. Physiol.* 2019;234(5):5379–5389.
35. Hwang SS, Lim J, Yu Z, et al. mRNA destabilization by BTG1 and BTG2 maintains T cell quiescence. *Science*. 2020;367(6483):1255–1260.
36. Cabeza-Arvelaiz Y, Sepulveda JL, Lebovitz RM, Thompson TC, Chinault AC. Functional identification of LZTS1 as a candidate prostate tumor suppressor gene on human chromosome 8p22. *Oncogene*. 2001;20(31):4169–4179.
37. Nam J-S, Hirohashi S, Wakefield LM. Dysadherin: a new player in cancer progression. *Cancer Lett.* 2007;255(2):161–169.
38. Desmots F, Roussel M, Pangault C, et al. Pan-HDAC Inhibitors Restore PRDM1 Response to IL21 in CREBBP-Mutated Follicular Lymphoma. *Clin. Cancer Res.* 2019;25(2):735–746.
39. Vega F, Medeiros LJ, Lang W-H, et al. The stromal composition of malignant lymphoid aggregates in bone marrow: variations in architecture and phenotype in different B-cell tumours. *British Journal of Haematology*. 2002;117(3):569–576.
40. Wahlin BE, Sander B, Christensson B, et al. Entourage: the immune microenvironment following follicular lymphoma. *Blood Cancer J*. 2012;2(1):e52.
41. Rajnai H, Bödör C, Balogh Z, et al. Impact of the reactive microenvironment on the bone marrow involvement of follicular lymphoma. *Histopathology*. 2012;60(6B):E66-75.
42. Peinado H, Alečković M, Lavotshkin S, et al. Melanoma exosomes educate bone marrow progenitor cells toward a pro-metastatic phenotype through MET. *Nature Medicine*. 2012;18(6):883–891.
43. Dai J, Escara-Wilke J, Keller JM, et al. Primary prostate cancer educates bone stroma through exosomal pyruvate kinase M2 to promote bone metastasis. *J. Exp. Med.* 2019;216(12):2883–2899.
44. Horiguchi H, Kobune M, Kikuchi S, et al. Extracellular vesicle miR-7977 is involved in hematopoietic dysfunction of mesenchymal stromal cells via poly(rC) binding protein 1 reduction in myeloid neoplasms. *Haematologica*. 2016;101(4):437–447.
45. Maswabi BCL, Molinsky J, Savvulidi F, et al. Hematopoiesis in patients with mature B-cell malignancies is deregulated even in patients with undetectable bone marrow involvement. *Haematologica*. 2017;102(4):e152–e155.
46. Manček-Keber M, Lainšček D, Benčina M, et al. Extracellular vesicle–mediated transfer of constitutively active MyD88L265P engages MyD88wt and activates signaling. *Blood*. 2018;131(15):1720–1729.
47. Liu W, Zhu M, Wang H, Wang W, Lu Y. Diffuse large B cell lymphoma-derived extracellular vesicles educate macrophages to promote tumours progression by increasing PGC-1β. *Scand. J. Immunol.* 2020;91(2):e12841.
48. Ferretti E, Tripodo C, Pagnan G, et al. The interleukin (IL)-31/IL-31R axis contributes to tumor growth in human follicular lymphoma. *Leukemia*. 2015;29(4):958–968.
49. Dörsam B, Bösl T, Reiners KS, et al. Hodgkin Lymphoma-Derived Extracellular Vesicles Change the Secretome of Fibroblasts Toward a CAF Phenotype. *Front Immunol*. 2018;9:1358.
50. Yang Z-Z, Grote DM, Ziesmer SC, et al. Soluble and Membrane-Bound TGF-β-Mediated Regulation of Intratumoral T Cell Differentiation and Function in B-Cell Non-Hodgkin Lymphoma. *PLOS ONE*. 2013;8(3):e59456.

51. Yang Z-Z, Grote DM, Xiu B, et al. TGF-β upregulates CD70 expression and induces exhaustion of effector memory T cells in B-cell non-Hodgkin's lymphoma. *Leukemia*. 2014;28(9):1872–1884.
52. Yan W, Li SX, Gao H, Yang W. Identification of B-cell translocation gene 1-controlled gene networks in diffuse large B-cell lymphoma: A study based on bioinformatics analysis. *Oncol Lett*. 2019;17(3):2825–2835.
53. Oricchio E, Nanjangud G, Wolfe AL, et al. The Eph-receptor A7 is a soluble tumor suppressor for follicular lymphoma. *Cell*. 2011;147(3):554–564.
54. Aung T, Chapuy B, Vogel D, et al. Exosomal evasion of humoral immunotherapy in aggressive B-cell lymphoma modulated by ATP-binding cassette transporter A3. *PNAS*. 2011;108(37):15336–15341.
55. Roccaro AM, Sacco A, Maiso P, et al. BM mesenchymal stromal cell-derived exosomes facilitate multiple myeloma progression. *J. Clin. Invest.* 2013;123(4):1542–1555.

FIGURE LEGENDS

Figure 1: FL B cells produced EVs that are internalized by BM-MSC and trigger their differentiation toward a FL-supportive stroma

A) Transmission electron microscopy of EVs harvested by ultracentrifugation of conditioned medium from RL B-cell line. Representative image of the data obtained with the different B-cell lines and primary FL B cells. **B**) Size analyse of EVs by Tunable Resistive Pulse Sensing (TRPS). Data are represented as the mean+/-SD from 6 (B-cell lines) or 4 (purified FL B cells) independent experiments. **C**) Quantification of EVs by TRPS after 48 h of culture of 10^4 B cells. **D**) Flow cytometry analysis of 1.5µM CellTrace Far Red-dyed EV uptake by BM-MSC after 6 hours in the presence or not of specific endocytosis inhibitors. Data are represented as the mean +/- SD of 4 independent experiments compared to the control condition (CTRL) arbitrary assigned at 100%. Statistical significance was evaluated before normalisation using the Dunnet post-hoc test. *** P<.001, * P<0.5. **E**) Purified primary FL B cells (n=8) were co-cultured (ratio 4:1) or not with BM-MSC pre-treated or not with FL-derived EVs for 3 days. After 2 days, the percentage of active Caspase-3^{pos} CD19/CD20^{pos} apoptotic malignant B cells was evaluated and was compared with that of malignant B cells cultured alone using a non-parametric Wilcoxon test. Each symbol represents a different FL patient * P<.05.

Figure 2: Comparison of the gene expression profile of BM-MSC primed by FL-derived EVs or TNF/LT

A) Venn diagram representing the number of genes upregulated and downregulated in HD BM-MSC (n=5) by FL-derived EVs from 3 different FL B-cell lines *versus* TNF/LT, as evaluated by RNAseq. **B**) Unsupervised principal component analysis (PCA) of Affymetrix GEP of FL-derived BM-MSC (FL_BM-MSC) (n=8) and FL-derived LN lymphoid stromal cells (FL_LN-LSC) (n=8). **C**) GSEA enrichment scores for the TNF/LT signature (1312 upregulated genes) and the EV signature (1218 upregulated genes) between FL_BM-MSC and FL_LN-LSC. **D-E**) Study of the EV signature using GO term enrichment analysis (D) and GSEA on REACTOME pathways (E). **F**) Comparison of the EV-primed BM-MSC and the TNF/LT-primed BM-MSC with the murine BM mesenchymal cells recently described by scRNASeq[25,26]. The assignment of the mouse BM stroma cell clusters restricted to

the mesenchymal compartments as described in these two studies is indicated in right.

Figure 3: Hematopoietic stem cell niche signature is enriched in EV-primed BM-MSC

A) Hierarchical clustering of untreated, TNF/LT primed, and EV-primed BM-MSC on selected differentially expressed genes as evaluated by RNAseq. The relative level of gene expression is depicted according to the shown color scale. **B**) qPCR validation of the RNAseq data on BM-MSC treated by FL-derived EVs (n=27) and TNF/LT (n=9) highlighting genes upregulated by EVs (left) or TNF:LT (right). Results are expressed as the fold change compared to untreated BM-MSC assigned at 1 (red dotted line). * P<.05, *** P<.001.

Figure 4: Characterization of the phenotype of BM-MSC treated by EVs purified from FL BM plasma

A) Representative image of transmission electron microscopy of EVs harvested by ultracentrifugation of HD BM plasma (upper) and FL BM plasma (bottom). **B**) Size analyse by Tunable Resistive Pulse Sensing (TRPS) of EVs harvested from HD BM plasma (upper, n=4) or FL BM plasma (bottom, n=4). Data are represented as the mean+/- SD. **C**) qPCR of BM-MSC treated by 15µL of EVs freshly enriched from BM plasma of healthy donor (n=6) and FL patients (n=13). Results expressed as fold change of untreated BM-MSC. * P<.05, ** P<.01. **D**) Luminex assay on BM plasma from HD BM (n=10) and FL BM (n=20). P<.05, ** P<.01, *** P<.001.

Figure 5: EV-induced signalization in BM-MSC

A) Analysis of transcription factor enrichment in the promoters of EV (left) or TNF/LT (right) upregulated genes performed with HOMER. Represented are significant motifs. **B**) Enrichment for transcription factor targets in EV (left) or TNF/LT (right) upregulated genes as determined with TRRUST database with EnrichR website. The Top20 enriched transcription factors were represented as dot plots. **C)** A TGF-β sensor cell line was stimulated overnight by TGF-β1, EVs from RL cell line (FL EVs), or pooled EVs from tonsil B cells (TONS EVs), in the presence or not of the TGFBR1 inhibitor galunisertib (Gal). GFP expression was determined by flow cytometry and expressed as the mean fluorescence intensity (MFI). Shown are 4 independent

experiments with one example of a representative data in histogram. **D)** Evaluation of SMAD2/3 and p38 phosphorylation by flow cytometry after a 6-hour stimulation by RL EVs. Shown is one representative experiment out of 3. **E**) Analysis by qPCR of BM-MSC (n=6) treated by RL EVs +/- TGFBR1 inhibition by galunisertib (Gal). Results expressed as median fold change of untreated BM-MSC. **F)** Analysis by qPCR of BM-MSC (n=6) treated by EVs from purified tonsil B cells. Results expressed as median fold change of untreated BM-MSC.

Figure 6: Characterization of BM FL B cell phenotype.

A) Unsupervised Pearson correlation clustering on all expressed genes in purified FL B cells from LN (n=10) and BM (n=5), including 3 paired BM/LN samples (FL1, FL2, and FL5). **B**) List of the Top10 GO terms associated with the two modules identified as correlated with the tissue origin of FL B cells by weighted gene co-expression network analysis (WGCNA). **C**) Heatmap of the differentially expressed genes between BM FL B cells and LN FL B cells (P <.01). **D**) GSEA analysis of the MSigDB hallmark pathways comparing BM FL B cells and LN FL B cells. **E**) qPCR validation of the downregulation of *MKI67* and *CKD1* in BM FL B cells (n=7) compared to LN FL B cells (n=10). Results are represented in arbitrary units obtained by assigning the value of 1 to a pool of PBMC. * P<.05, **P<.01

Figure 7: Characterization of the of the BM FL B cells interaction with stromal cells.

A) Purified FL B cells (n=4) were co-cultured with BM-MSC pre-treated by TNF/LT or FL-derived EVs for 3 days. At day 3, CD19/CD20^{pos} viable B cells were analyzed by flow cytometry for CD86 membrane expression (left, expressed as a ratio of mean fluorescence intensity compared to B cells co-cultured on untreated BM-MSC) and Ki67 nuclear expression (right, expressed as a percentage of stained B cells). **B**) Circos plots showing predicted interactions between BM-MSC defined as sender cells and FL B cells defined as receiver cells based on the genes enriched in the EV signature and/or the TNF/LT signature compared to untreated BM-MSC and on the genes enriched in BM FL B cells (left) or LN FL B cells (right) compared to normal centrocytes.

FIGURE 1

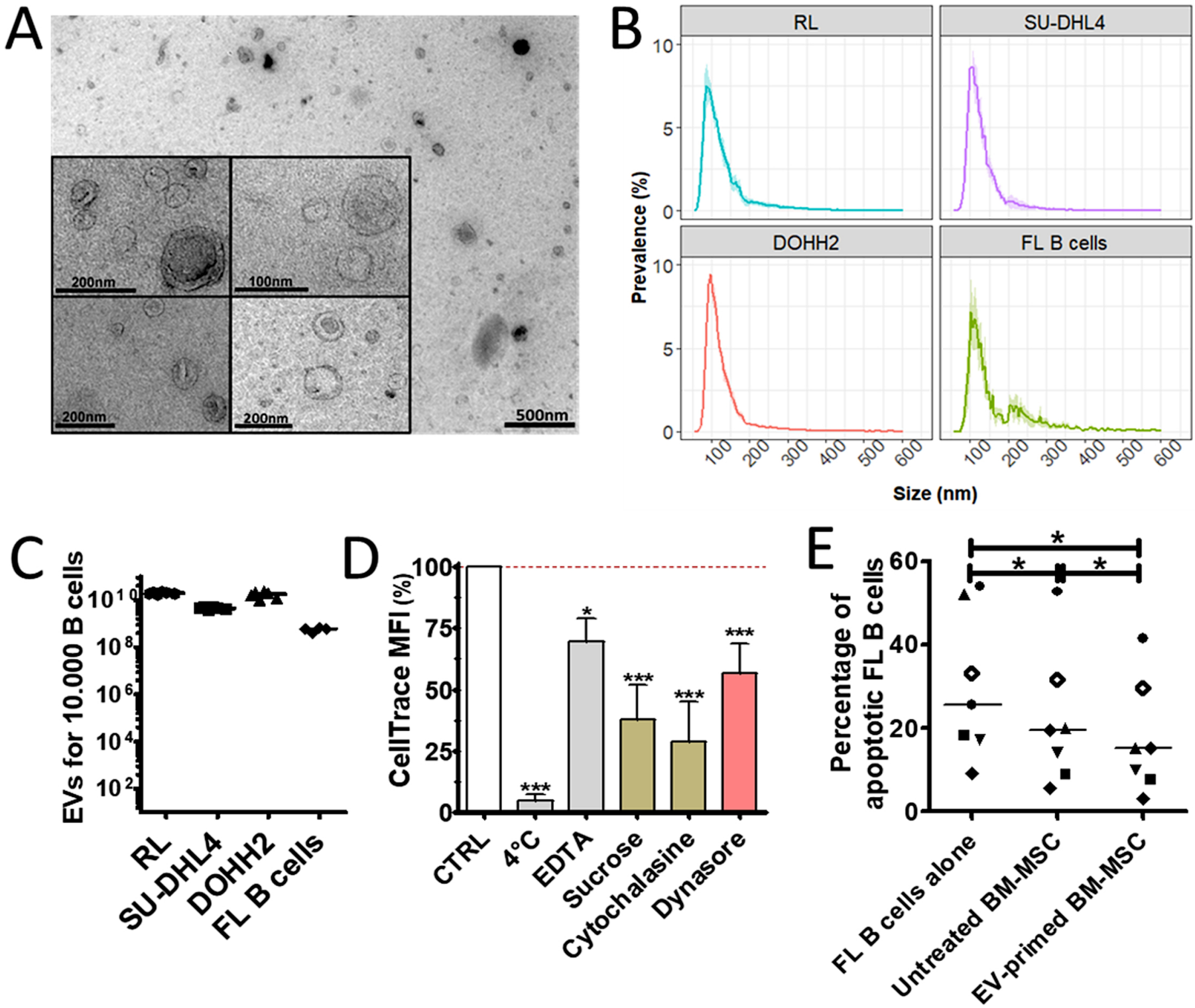
A
200nm
100nm
200nm
200nm
500nm
B
RL
SU-DHL4
DOHH2
FL B cells
Prevalence (%)
Size (nm)
C
EVs for 10.000 B cells
RL
SU-DHL4
DOHH2
FL B cells
D
CellTrace MFI (%)
CTRL
4°C
EDTA
Sucrose
Cytochalasine
Dynasore
E
Percentage of apoptotic FL B cells
FL B cells alone
Untreated BM-MSC
EV-primed BM-MSC

FIGURE 2

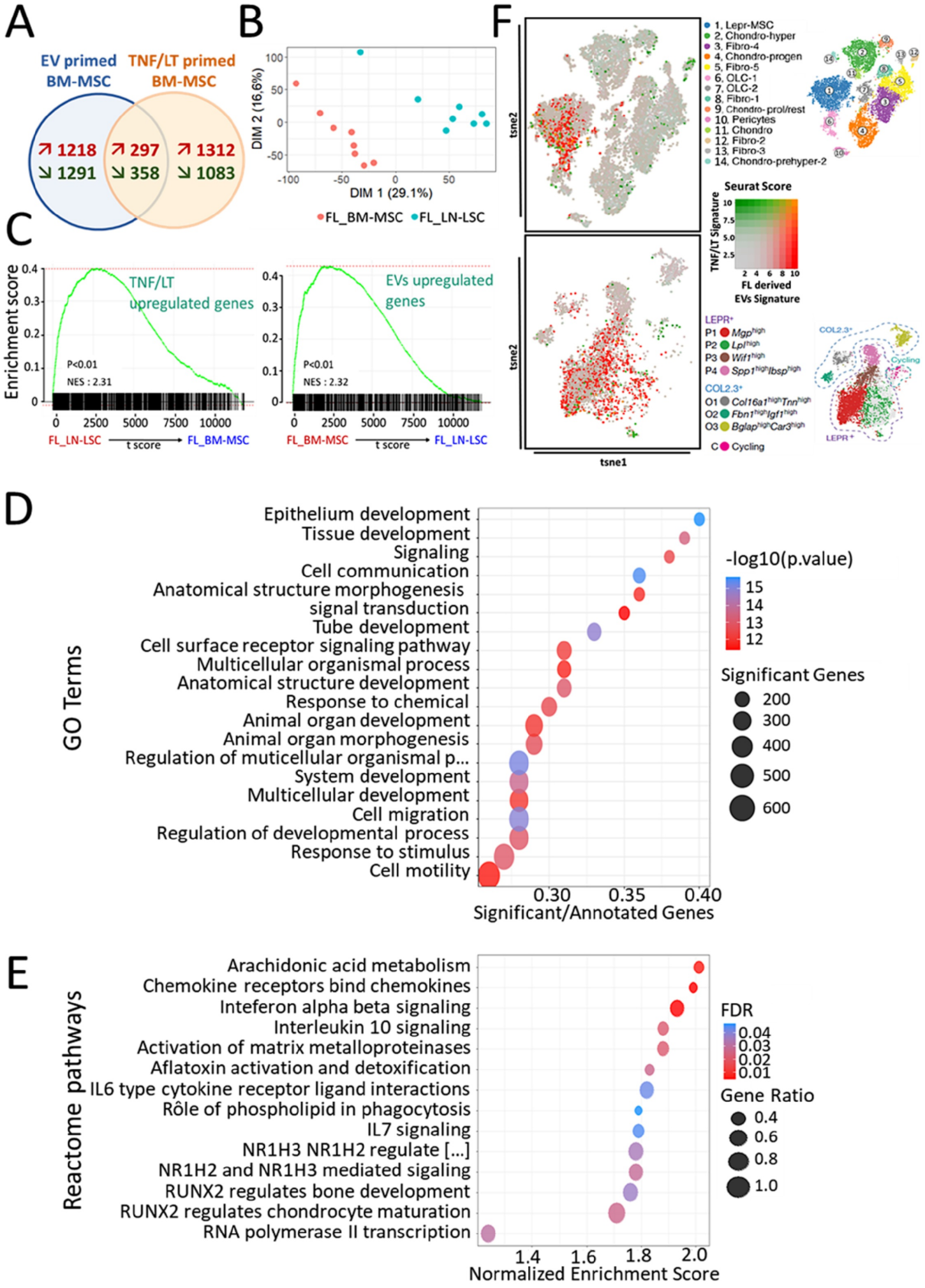
A
EV primed BM-MSC
TNF/LT primed BM-MSC
↗ 1218
↘ 1291
↗ 297
↘ 358
↗ 1312
↘ 1083
B
DIM 2 (16,6%)
DIM 1 (29.1%)
FL_BM-MSC
FL_LN-LSC
C
Enrichment score
TNF/LT upregulated genes
P<0.01
NES : 2.31
FL_LN-LSC
t score
FL_BM-MSC
EVs upregulated genes
P<0.01
NES : 2.32
FL_BM-MSC
t score
FL_LN-LSC
F
tsne2
tsne1
1. Lepr-MSC
2. Chondro-hyper
3. Fibro-4
4. Chondro-progen
5. Fibro-5
6. OLC-1
7. OLC-2
8. Fibro-1
9. Chondro- prol/rest
10. Pericytes
11. Chondro
12. Fibro-2
13. Fibro-3
14. Chondro-prehyper-2
Seurat Score
TNF/LT Signature
FL derived EVs Signature
LEPR+
P1 Mgp high
P2 Lpl high
P3 Wif1 high
P4 Spp1 high Ibsp high
COL2.3+
O1 Col16a1 high Tnn high
O2 Fbn1 high Igf1 high
O3 Bglap high Car3 high
C Cycling
COL2.3+
Cycling
LEPR+
D
GO Terms
Epithelium development
Tissue development
Signaling
Cell communication
Anatomical structure morphogenesis
signal transduction
Tube development
Cell surface receptor signaling pathway
Multicellular organismal process
Anatomical structure development
Response to chemical
Animal organ development
Animal organ morphogenesis
Regulation of muticellular organismal p...
System development
Multicellular development
Cell migration
Regulation of developmental process
Response to stimulus
Cell motility
Significant/Annotated Genes
-log10(p.value)
Significant Genes
E
Reactome pathways
Arachidonic acid metabolism
Chemokine receptors bind chemokines
Inteferon alpha beta signaling
Interleukin 10 signaling
Activation of matrix metalloproteinases
Aflatoxin activation and detoxification
IL6 type cytokine receptor ligand interactions
Rôle of phospholipid in phagocytosis
IL7 signaling
NR1H3 NR1H2 regulate [...]
NR1H2 and NR1H3 mediated sigaling
RUNX2 regulates bone development
RUNX2 regulates chondrocyte maturation
RNA polymerase II transcription
Normalized Enrichment Score
FDR
Gene Ratio

FIGURE 3

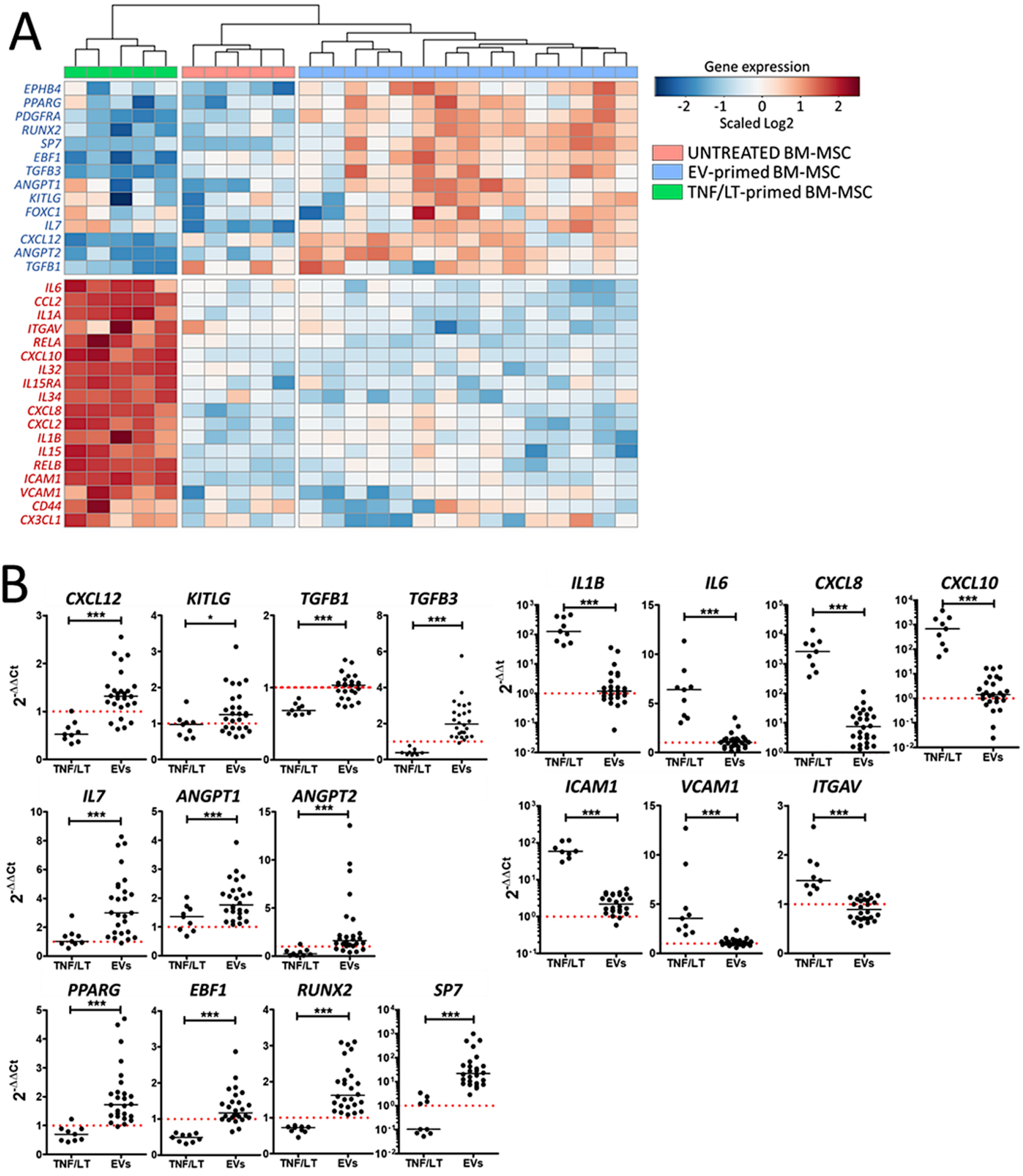

FIGURE 4

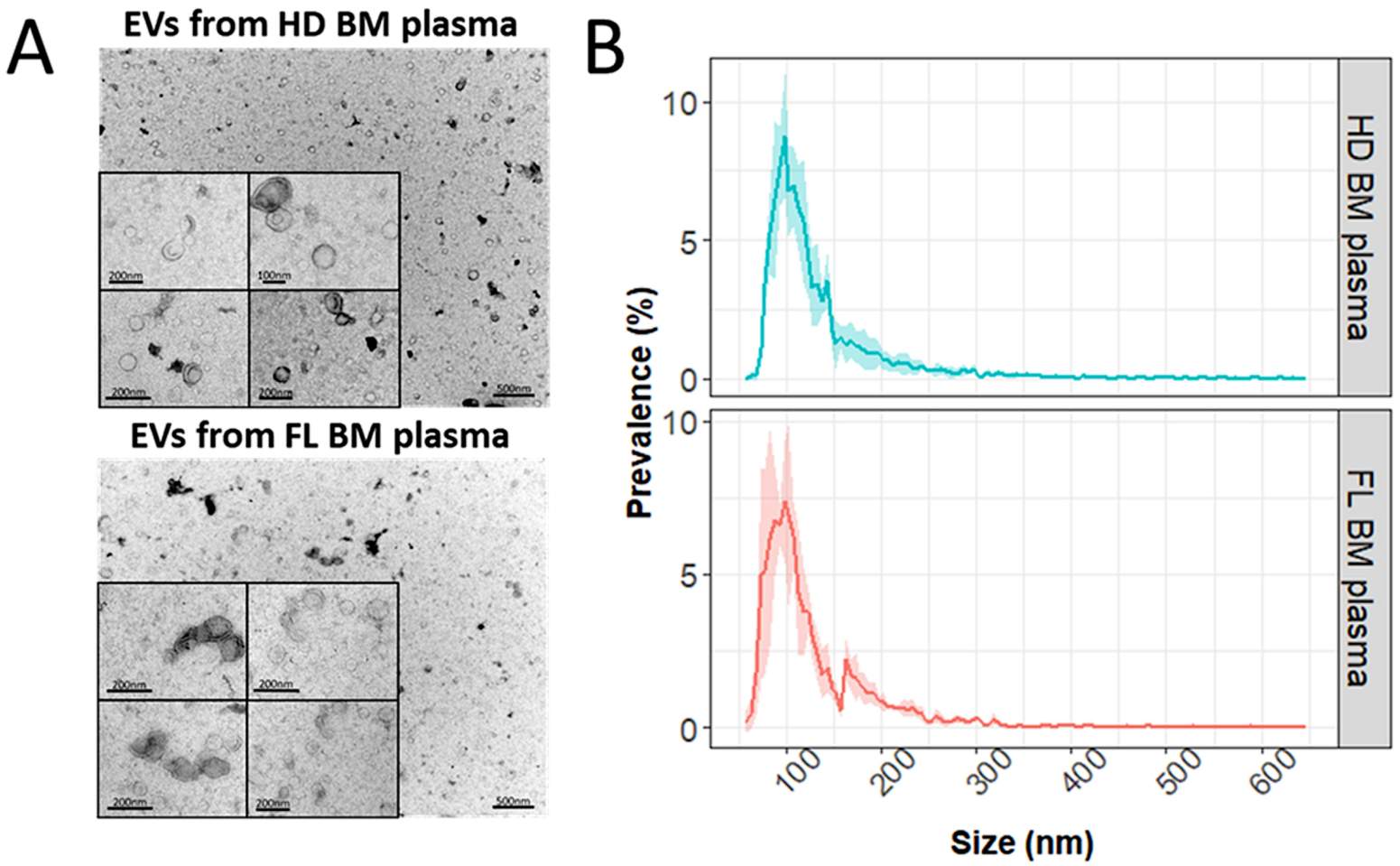

FIGURE 5

A

EV signature

RANK	MOTIF	SYMBOL	P-VALUE
1		SOX6	1,00E-04
2		SOX2	1,00E-03
3		SOX21	1,00E-03
4		SOX4	1,00E-03
5		SOX10	1,00E-03

TNF/LT signature

RANK	MOTIF	SYMBOL	P-VALUE
1	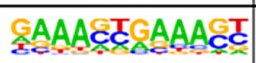	IRF2	1,00E-13
2		IRF1	1,00E-12
3		IRF3	1,00E-09
4		IRF8	1,00E-07
5		NFkB-p65	1,00E-07
6		PRDM1	1,00E-03
7		IRF4	1,00E-03

B

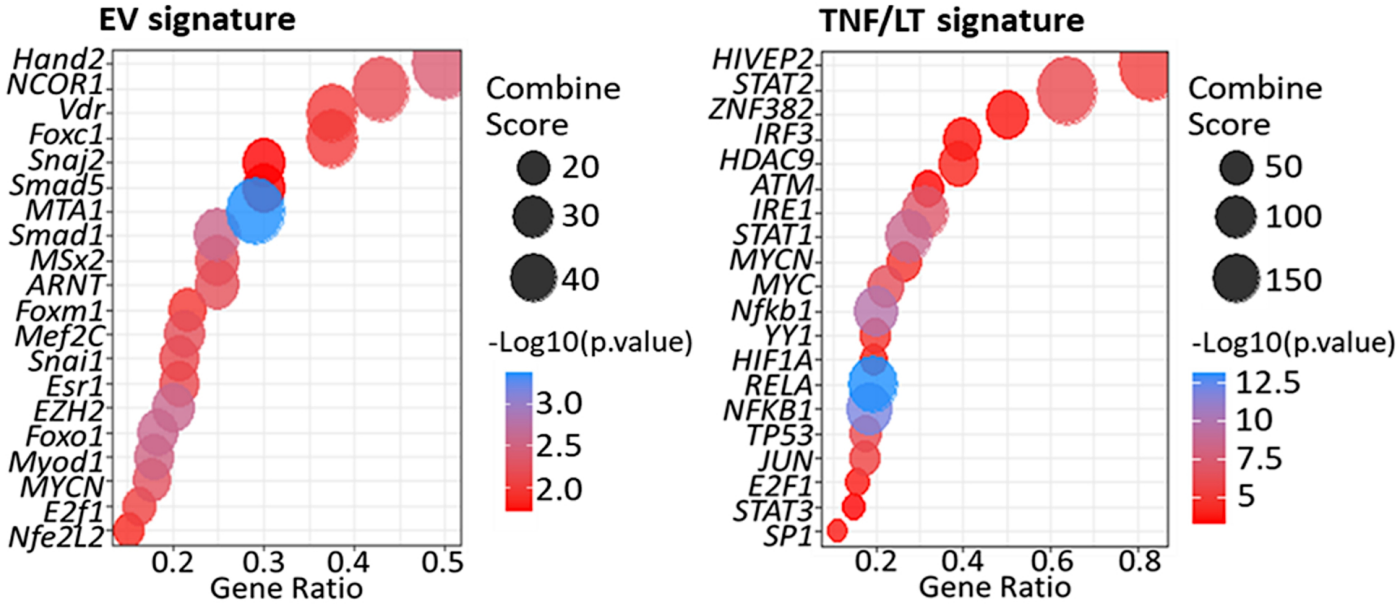

C

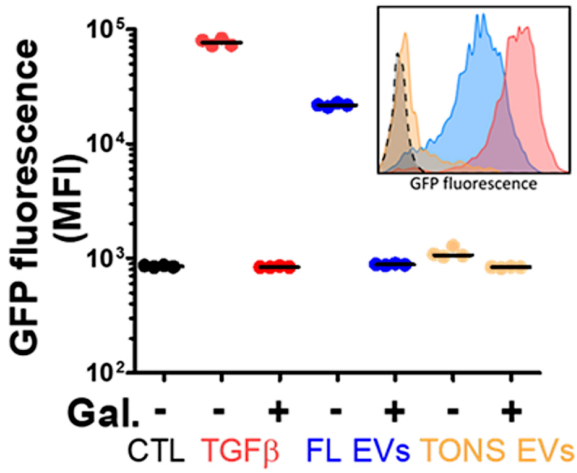

D

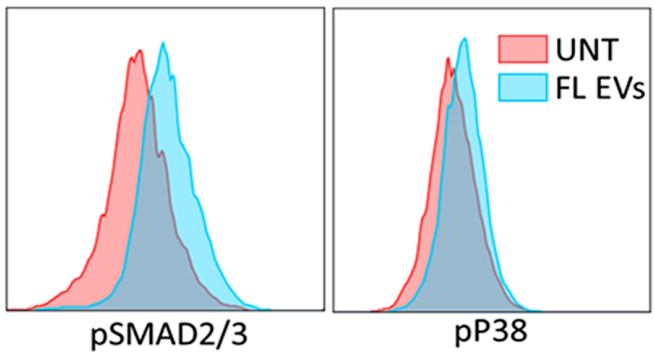

E

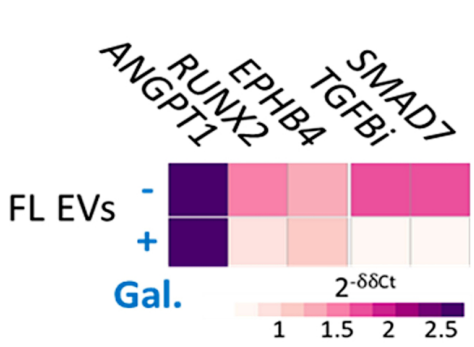

F

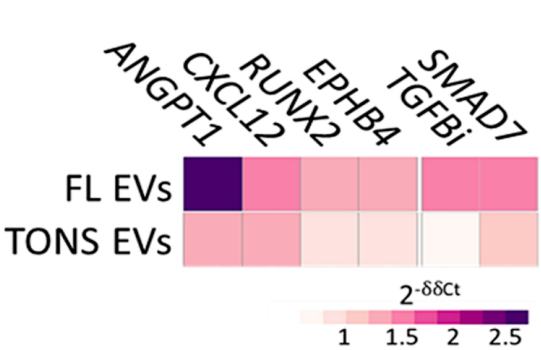

FIGURE 6

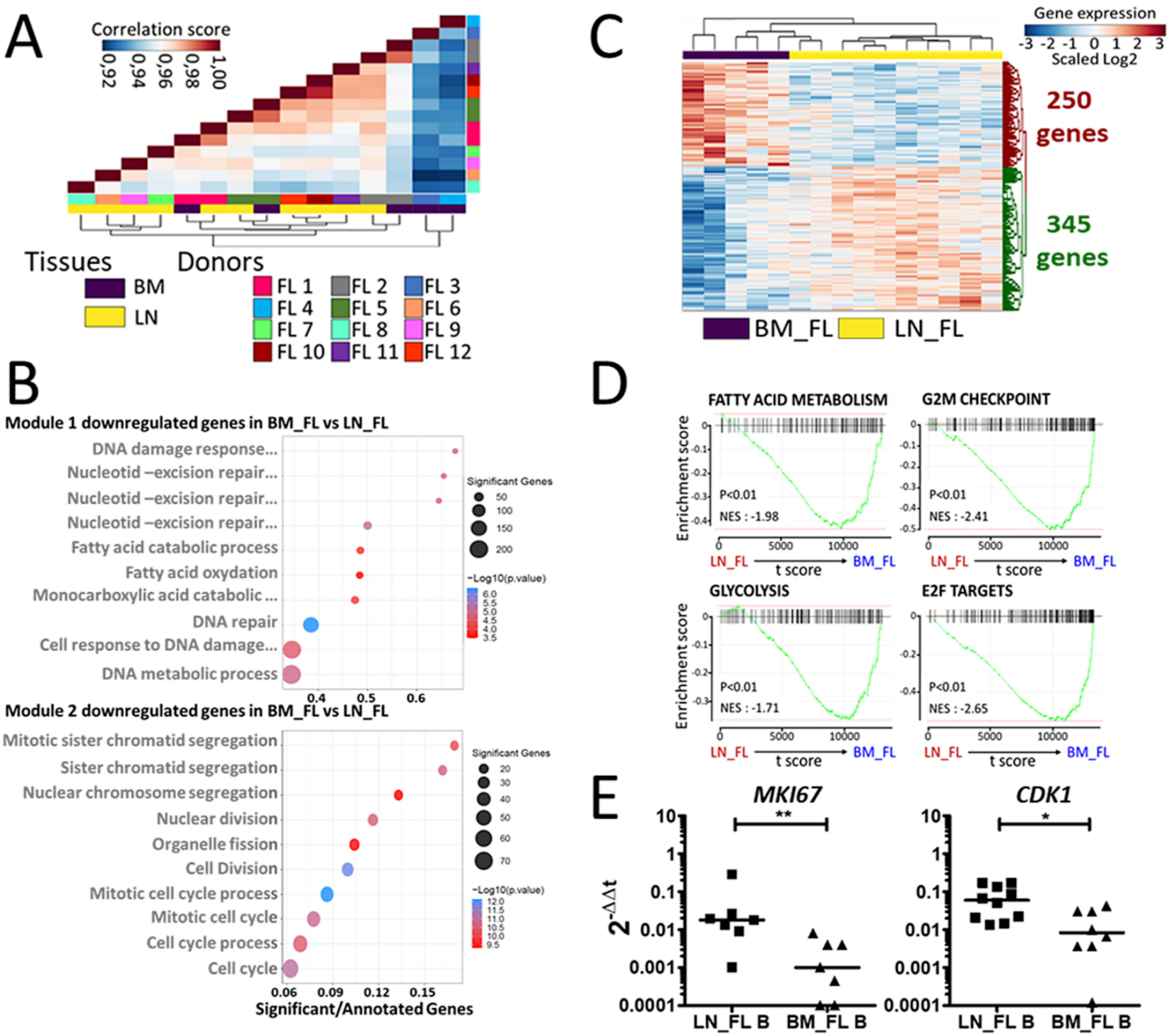
A
Correlation score
0,92
0,94
0,96
0,98
1,00
Tissues
Donors
BM
LN
FL 1
FL 2
FL 3
FL 4
FL 5
FL 6
FL 7
FL 8
FL 9
FL 10
FL 11
FL 12
B
Module 1 downregulated genes in BM_FL vs LN_FL
DNA damage response...
Nucleotid –excision repair...
Nucleotid –excision repair...
Nucleotid –excision repair...
Fatty acid catabolic process
Fatty acid oxydation
Monocarboxylic acid catabolic ...
DNA repair
Cell response to DNA damage...
DNA metabolic process
0.4
0.5
0.6
Significant Genes
50
100
150
200
-Log10(p.value)
6.0
5.5
5.0
4.5
4.0
3.5
Module 2 downregulated genes in BM_FL vs LN_FL
Mitotic sister chromatid segregation
Sister chromatid segregation
Nuclear chromosome segregation
Nuclear division
Organelle fission
Cell Division
Mitotic cell cycle process
Mitotic cell cycle
Cell cycle process
Cell cycle
0.06
0.09
0.12
0.15
Significant/Annotated Genes
Significant Genes
20
30
40
50
60
70
-Log10(p.value)
12.0
11.5
11.0
10.5
10.0
9.5
C
Gene expression
-3 -2 -1 0 1 2 3
Scaled Log2
250
genes
345
genes
BM_FL
LN_FL
D
FATTY ACID METABOLISM
G2M CHECKPOINT
GLYCOLYSIS
E2F TARGETS
Enrichment score
P<0.01
NES : -1.98
NES : -2.41
NES : -1.71
NES : -2.65
LN_FL
t score
BM_FL
E
MKI67
CDK1
**
*
2-ΔΔt
LN_FL B
BM_FL B

FIGURE 7

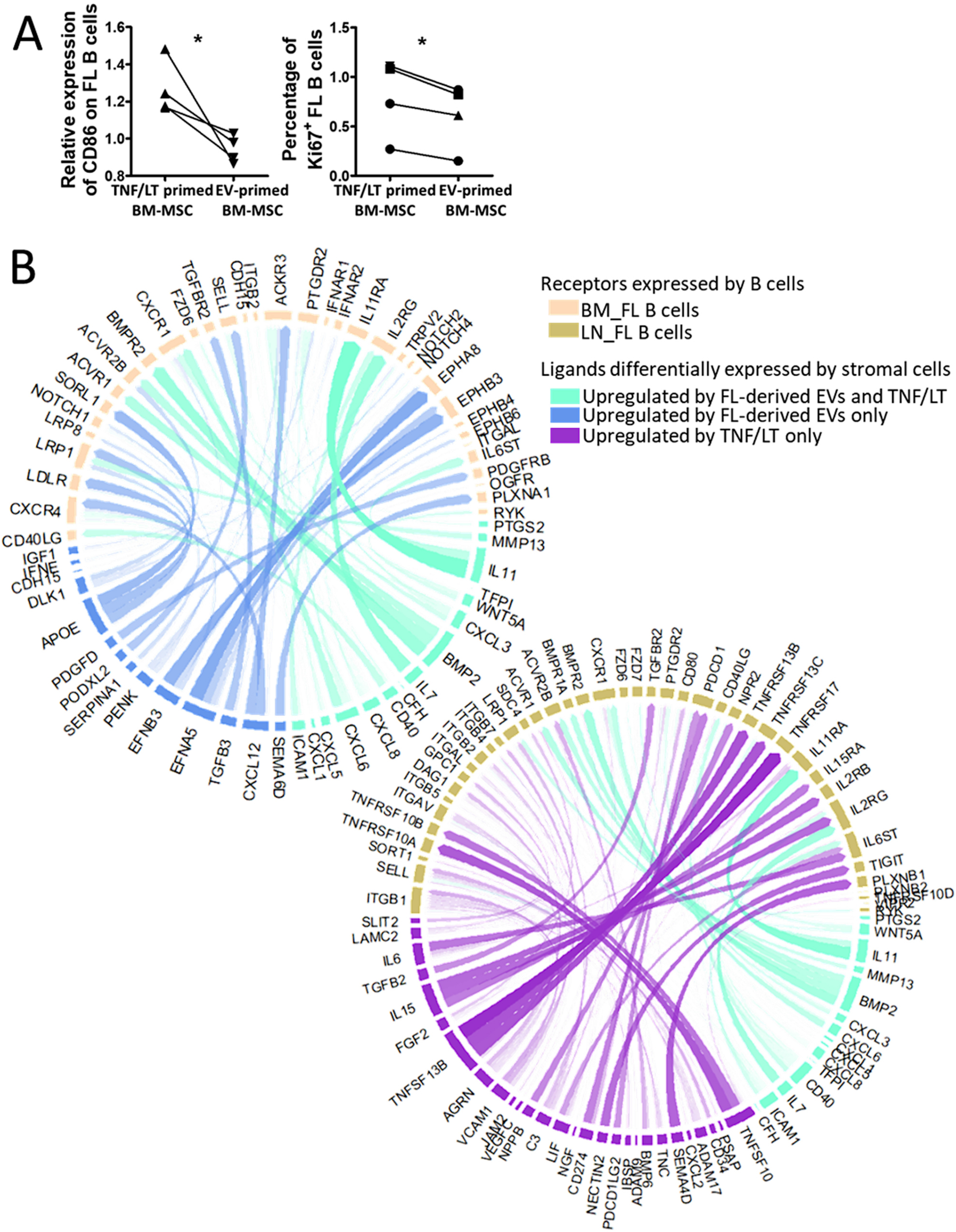
A
Relative expression of CD86 on FL B cells
1.6
1.4
1.2
1.0
0.8
*
TNF/LT primed BM-MSC
EV-primed BM-MSC
Percentage of Ki67+ FL B cells
1.5
1.0
0.5
0.0
*
TNF/LT primed BM-MSC
EV-primed BM-MSC
B
Receptors expressed by B cells
BM_FL B cells
LN_FL B cells
Ligands differentially expressed by stromal cells
Upregulated by FL-derived EVs and TNF/LT
Upregulated by FL-derived EVs only
Upregulated by TNF/LT only